Key role of tissue plasminogen activator in neurovascular coupling

Laibaik Park*, Eduardo F. Gallo*, Josef Anrather*, Gang Wang*, Erin H. Norris†, Justin Paul†, Sidney Strickland†, and Costantino Iadecola*‡

*Division of Neurobiology, Department of Neurology and Neuroscience, Weill Medical College of Cornell University, New York, NY 10021; and †Laboratory of Neurobiology and Genetics, The Rockefeller University, New York, NY 10021

The increase in blood flow evoked by synaptic activity is essential for normal brain function and underlies functional brain imaging signals. Nitric oxide, a vasodilator released by NMDA receptor activation, is critical for the flow increase, but the factors linking NMDA receptor activity to nitric oxide-dependent hyperemia are poorly understood. Here, we show that tissue plasminogen activator (tPA), a serine protease implicated in NMDA receptor signaling, is required for the flow increase evoked by somatosensory stimulation. tPA acts by facilitating neuronal nitric oxide release, but this effect does not involve enhancement of NMDA currents or the associated intracellular Ca²⁺ rise. Rather, the evidence suggests that tPA controls NMDA-dependent nitric oxide synthesis by influencing the phosphorylation state of neuronal nitric oxide synthase. These findings unveil a previously unrecognized role of tPA in vital homeostatic mechanisms coupling NMDA receptor signaling with nitric oxide synthesis and local cerebral perfusion.

calcium | cerebral blood flow | mouse | nitric oxide | phosphorylation

Tissue plasminogen activator (tPA) is a serine protease best known for its role in intravascular fibrinolysis (1–3). tPA converts plasminogen (plg) into plasmin, a protease that cleaves fibrin and dissolves newly formed clots (2). The ''clot-busting'' properties of tPA have been used successfully in the treatment of myocardial infarction and ischemic stroke (4, 5). In addition to its role in fibrinolysis, tPA has recently emerged as a pleiotropic neuromodulator implicated in various aspects of brain function (6). tPA is stored in neurons and is released in an activity-dependent manner via exocytosis (7, 8). tPA is involved in neurotransmission, synaptic plasticity, dendritic remodeling, and sympathetic nerve activity, effects related to its ability to influence NMDA receptor function, extracellular matrix integrity, and neurotransmitter release (9–15). In addition, tPA released from endothelial cells modulates cerebrovascular tone and may contribute to the hemodynamic changes induced by brain ischemia and trauma (3, 16–18).

The vascular effects of tPA and its involvement in synaptic function raise the possibility that this protease also contributes to the neurovascular mechanisms linking brain activity to cerebral blood flow (CBF). The brain lacks energy reserves and its integrity depends on a continuous supply of oxygen and glucose through CBF (19). Because of such dependence on CBF, the brain is endowed with complex regulatory mechanisms that match local cerebral perfusion to the energy needs of active neurons on a moment-to-moment basis (19). Thus, an increase in regional brain activity is associated with a rapid and spatially focused increase in CBF, a response termed ''functional hyperemia'' (19, 20). The close temporal and spatial correspondence between brain activity and CBF constitutes the basis of functional brain imaging techniques that use the local hemodynamic response evoked by neural activity to localize brain function (21).

The factors driving functional hyperemia are not well understood. Accumulating evidence suggests that the CBF changes are initiated by postsynaptic events triggered by activation of gluta-mate receptors and leading to release of vasoactive agents from neurons and astrocytic endfeet (20, 22). Although several agents contribute to vascular response evoked by neural activity (19), a large component of the hyperemia is mediated by NMDA receptors via the release of the potent vasodilator nitric oxide (NO) (23–25). Activation of NMDA receptors increases intracellular Ca²⁺, which activates neuronal NO synthase (nNOS), a Ca²⁺-calmodulin-dependent enzyme associated with the NMDA receptor complex through the scaffolding protein postsynaptic density-95 (PSD-95) (26, 27). NMDA receptors may influence nNOS activity also by regulating the phosphorylation of this enzyme (28–30). However, the factors linking NMDA receptor activity to NO synthesis and to the resulting increase in CBF have not been established.

Considering the prominent role that tPA plays in NMDA receptor signaling (6, 13, 15), we asked whether tPA participates in the mechanisms of functional hyperemia. We found that tPA is critical for the full expression of the flow increase evoked by activation of the mouse whisker barrel cortex. This effect is mediated by promoting NO synthesis during NMDA receptor activation. tPA does not increase nNOS activity by enhancing NMDA receptor currents and the associated rise in intracellular Ca²⁺, but it regulates NO production by influencing the phosphorylation state of nNOS. The findings establish tPA as a key factor in postsynaptic events linking NMDA receptor activation to NO synthesis and functional hyperemia.

Results

tPA Is Required for the Full Expression of Functional Hyperemia. To investigate the role of tPA in functional hyperemia, we examined the CBF increase produced by activation of the whisker barrel cortex in tPA-deficient mice (31). The facial whiskers were mechanically stimulated in anesthetized mice in which CBF was monitored in the contralateral whisker barrel cortex by laser Doppler flowmetry (32, 33). We found that the CBF increase evoked by whisker stimulation is markedly attenuated in tPA⁻/⁻ compared with wild-type mice (Fig. 1 a and b). Such attenuation was not a consequence of a generalized reduction of cerebrovascular reactivity because the CBF increase produced by the NO donor S-nitroso-D-penicillamine (SNAP) or by adenosine, agents that directly relax vascular smooth muscles, was not reduced [supporting information (SI) Fig. 6 a and b]. Similarly,
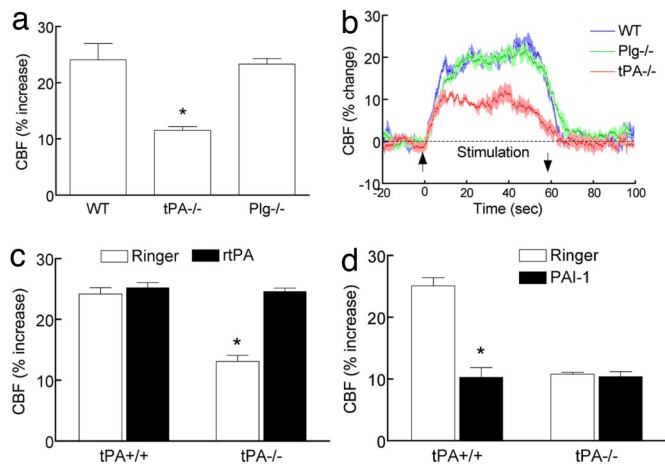
NEUROSCIENCE

Fig. 1. Functional hyperemia is attenuated in tPA$^{-/-}$ mice. (*a* and *b*) The increase in CBF produced by whisker stimulation is less in tPA$^{-/-}$ mice than in wild-type mice (WT) or plasminogen-null mice (Plg$^{-/-}$). (*c*) rtPA (20 μg/ml) rescues the attenuation in functional hyperemia in tPA$^{-/-}$ mice. (*d*) PAI-1 (1 μg/ml) attenuates functional hyperemia only in tPA$^{+/+}$ mice. *, $P < 0.05$ from WT and Plg$^{-/-}$; ANOVA and Tukey's test; $n = 5$ per group.

Fig. 2. Spontaneous and evoked neural activity is not altered in tPA-null mice. (*a*) The field potentials evoked by whisker activation are comparable in tPA$^{+/+}$ and tPA$^{-/-}$ mice. The arrow indicates the application of the stimulus. (*b*) The amplitude of the negative wave of the field potentials (asterisk in *a*) does not differ between tPA$^{+/+}$ and tPA$^{-/-}$ mice ($P > 0.05$, *t* test). (*c* and *d*) The amplitude and frequency distribution of neocortical electrical activity are nearly identical in tPA$^{+/+}$ and tPA$^{-/-}$ mice ($n = 5$ per group).

the increase in CBF produced by systemic hypercapnia, a potent vasoactive stimulus, was not attenuated in tPA$^{-/-}$ mice (SI Fig. 6c). tPA is also released from endothelial cells and can produce vasodilation (16, 18). However, the CBF increase produced by neocortical application of the endothelium-dependent vasodilators acetylcholine, bradykinin, or the Ca^{2+} ionophore A23187 was not reduced in tPA-null mice (SI Fig. 6 *d–f*), excluding a participation of tPA in endothelium-dependent vasodilation. Thus, tPA is involved specifically in the hemodynamic response initiated by neural activity.

To confirm that the reduction in functional hyperemia is caused by tPA deficiency, we examined whether exogenous tPA could rescue the CBF response to somatosensory activation in tPA$^{-/-}$ mice. Topical neocortical application of recombinant tPA (rtPA) did not affect cerebrovascular responses in tPA$^{+/+}$ mice (Fig. 1c and SI Fig. 7 *a–c*), but it fully reestablished the increase in CBF evoked by whisker stimulation in tPA$^{-/-}$ mice (Fig. 1c). rtPA did not alter resting CBF and the increase in CBF produced by acetylcholine or adenosine in tPA$^{-/-}$ mice (SI Fig. 7 *a–c*), ruling out that the rescue of functional hyperemia was the results of a nonspecific enhancement of vascular reactivity. To provide further evidence that endogenous tPA is involved in functional hyperemia and to rule out confounding compensatory changes in tPA$^{-/-}$ mice, we examined the effect of the plg activator inhibitor-1 (PAI-1), an endogenous inhibitor of tPA (2). In wild-type mice, neocortical superfusion with PAI-1 attenuated the CBF increase produced by whisker stimulation without affecting resting CBF or the CBF response to acetylcholine or adenosine (Fig. 1d and SI Fig. 7 *d–f*). Furthermore, PAI-1 did not attenuate functional hyperemia in tPA$^{-/-}$ mice, attesting to the specificity of its action (Fig. 1d). These data with PAI-1, in concert with the findings in tPA-null mice, demonstrate that tPA is essential for the full expression of the increase in CBF evoked by neural activity.

The Effect of tPA Is Independent of Plasmin and Cannot Be Attributed to Modulation of Neural Activity. Some of the effects of tPA are mediated by the protease plasmin, the main product of tPA proteolytic activity (1, 6). To examine whether plasmin is involved in the effect of tPA on functional hyperemia, we used mice lacking plg (34). We found that the increase in CBF produced by whisker stimulation, and other cerebrovascular responses as well, are not attenuated in plg$^{-/-}$ mice (Fig. 1 *a* and
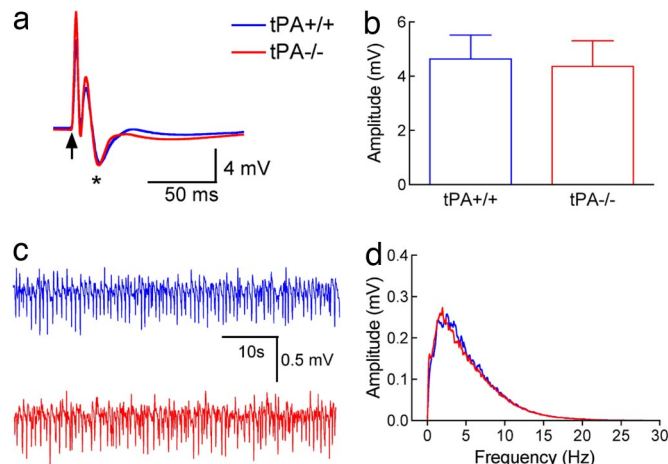
b and SI Fig. 6 *a–f*). Furthermore, tPA could contribute to functional hyperemia by enhancing the neural activity evoked by whisker stimulation. To examine this possibility we recorded spontaneous and evoked neural activity in wild-type and tPA-null mice. We found that the amplitude and frequency distribution of the electrocorticogram and the amplitude of the somatosensory field potentials produced by activation of the whisker pad do not differ between tPA$^{+/+}$ and tPA$^{-/-}$ mice (Fig. 2 *a–d*). Therefore, tPA does not contribute to functional hyperemia by activating plg or by modulating the neural activity evoked by whisker stimulation.

tPA Is Involved Only in the Increase in CBF Triggered by Activation of NMDA Receptors. Functional hyperemia in the neocortex depends in large part on activation of NMDA receptors (23, 35). Because tPA can modulate NMDA receptor function (6, 13, 15), we asked whether the effect of tPA on the hyperemic response depends on NMDA receptors. We reasoned that, if tPA acts through NMDA receptors, then its effect on functional hyperemia should be prevented by the NMDA receptor inhibitor MK801. We found that MK801 attenuates the CBF response induced by whisker stimulation in tPA$^{+/+}$ mice but not in tPA$^{-/-}$ mice (Fig. 3a). In contrast, the sodium channel blocker tetrodotoxin (TTX) attenuated the CBF response in tPA-null mice (Fig. 3a), without altering resting CBF or other cerebrovascular responses (SI Fig. 8 *a–c*). Thus, the lack of effect of MK801 in tPA nulls is not due to the fact that the response is already maximally reduced. However, the data with MK801 do not demonstrate a direct link between tPA and NMDA receptors. To investigate more directly the role of tPA on NMDA-dependent hyperemia, we examined the cerebrovascular effects of neocortical application of NMDA. The increase in CBF produced by topical NMDA was markedly attenuated in tPA$^{-/-}$ mice (Fig. 3b), whereas responses to AMPA (Fig. 3c) and kainate (SI Fig. 8d) were not reduced. Thus, tPA is exclusively involved in the component of the increase in CBF mediated by activation of NMDA receptors.

tPA Modulates the NO Release Elicited by Activation of NMDA Receptors. The hyperemia evoked by NMDA receptor activation is mediated by NO produced by nNOS (36–38). Therefore, we tested the hypothesis that tPA contributes to functional hyper-
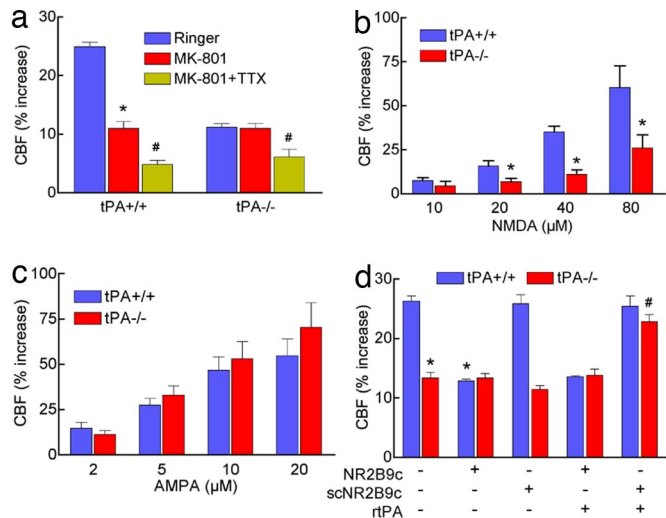
Fig. 3. tPA is selectively involved in the hyperemia induced by NMDA. (*a*) MK801 (10 μM) attenuates functional hyperemia only in tPA$^{+/+}$ mice, but TTX (3 μM) attenuates the response in both tPA$^{+/+}$ and tPA$^{-/-}$ mice; ∗, $P < 0.05$ from vehicle; #, $P < 0.05$ from vehicle and MK801; ANOVA and Tukey's test; $n =$ 5 per group. (*b*) The increase in CBF produced by topical application of NMDA is attenuated in tPA$^{-/-}$ mice. ∗, $P < 0.05$ from tPA$^{+/+}$; $n = 5$ per group. (*c*) The increase in CBF produced by topical application of AMPA is not attenuated in tPA$^{-/-}$ mice; $P > 0.05$; $n = 5$ per group. (*d*) PSD-95 is involved in the effect of tPA on functional hyperemia. NR2B9c (20 μM), a peptide that inhibits the association of NR2 with PSD-95, attenuates functional hyperemia in tPA$^{+/+}$ but not tPA$^{-/-}$ mice. The control peptide scNR2B9c (20 μM), which does not interact with NR2, has no effect. NR2B9c, but not scNR2B9c, prevents exogenous rtPA from rescuing functional hyperemia in tPA$^{-/-}$ mice. ∗, $P < 0.05$ from tPA$^{+/+}$; #, $P < 0.05$ from tPA$^{-/-}$ and $P > 0.05$ from tPA$^{+/+}$; $n = 5$ per group.

emia by promoting NO synthesis from nNOS linked to postsynaptic NMDA receptors. In the postsynaptic density, the NR2 subunit of the NMDA receptor is linked to nNOS through the PSD-95/Discs large/zona occludens-1 (PDZ) domains of the scaffolding protein PSD-95 (39). Disruption of the link between NR2B and PSD-95 uncouples NMDA receptor activity from NO production without altering NMDA currents and the related increase in intracellular Ca^{2+} (40, 41). To determine whether tPA is involved in the component of functional hyperemia mediated by postsynaptic NMDA receptors linked to nNOS, we used a cell-permeable peptide inhibitor (NR2B9c) (41, 42). This peptide binds to the PDZ domain of NR2B and disrupts its association with the PSD-95–nNOS complex (41, 42). First, we established whether the increase in CBF evoked by neural activity depends on the NMDA receptor–nNOS complex via PSD-95. Pretreatment of the cranial window with NR2B9c, but not with a control peptide not interacting with NR2B (scNR2B9c) (42), attenuated the increase in CBF produced by whisker stimulation (Fig. 3*d*), without affecting resting CBF and other cerebrovascular responses (SI Fig. 9 *a–c*). Thus, disruption of the link between NMDA receptors and nNOS attenuates functional hyperemia, indicating a specific involvement of postsynaptic NMDA receptors and excluding the participation of NMDA receptors on other cells. Next, we tested whether the association between the NMDA receptor and nNOS is needed for the effects of tPA on functional hyperemia. If so, the peptide inhibitor should prevent the rescue of the CBF response by exogenous tPA in tPA$^{-/-}$ mice. In agreement with this prediction, rtPA failed to reconstitute the response to whisker stimulation in tPA-null mice treated with NR2B9c, but not in null mice treated with the inactive peptide scNR2B9c (Fig. 3*d*). These findings suggest that disruption of the interaction between the NMDA receptor and nNOS prevents the action of tPA on
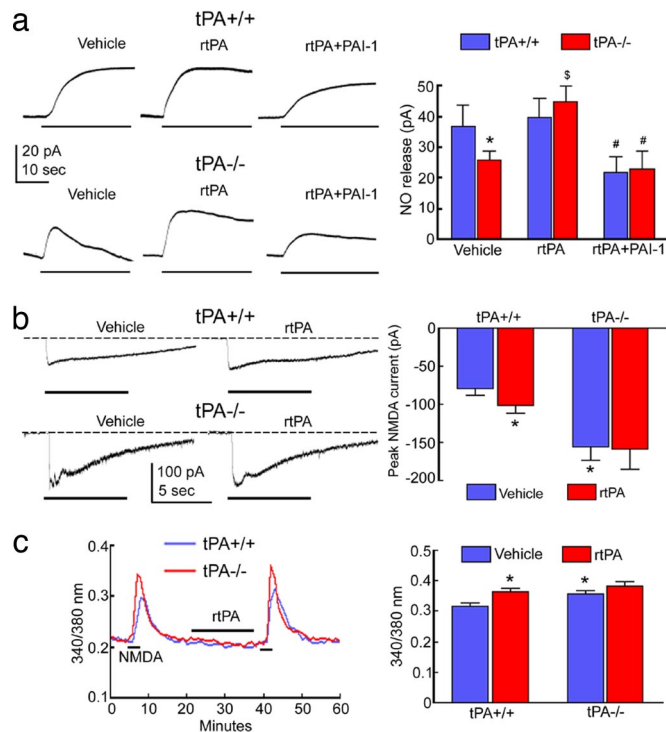

Fig. 4. tPA is required for NMDA-dependent NO production. (*a*) NMDA-induced (30 μM) NO release is attenuated in tPA$^{-/-}$ mice, a reduction counteracted by rtPA (20 μg/ml). PAI-1 (1 μg/ml) attenuates NO release in tPA$^{+/+}$ mice and in tPA$^{-/-}$ mice treated with rtPA; ∗, $P < 0.05$ from tPA$^{+/+}$ vehicle; \$, $P < 0.05$ from tPA$^{-/-}$ vehicle; #, $P < 0.05$ from respective genotype in rtPA-treated group; ANOVA and Tukey's test; $n = 6–8$ per group. (*b*) NMDA currents are not attenuated in tPA$^{-/-}$ mice, but are larger; ∗, $P < 0.05$ from tPA$^{+/+}$ vehicle; $n = 6–8$ per group. (*c*) Increase in intracellular Ca^{2+} evoked by NMDA is not attenuated in tPA$^{-/-}$ mice, but is larger; ∗, $P < 0.05$ from tPA$^{+/+}$ vehicle; $n = 20–30$ per group.

functional hyperemia. To examine more directly whether tPA is involved in nNOS-dependent NO synthesis, we studied the effect of tPA on NO release in cortical neuronal cultures by using NO-sensitive microelectrodes. In wild-type cultures, NMDA induced a dose-dependent increase in the NO signal that was blocked by MK801 and markedly attenuated by the NOS inhibitor L-NNA, attesting to the validity of the measurement (SI Fig. 10 *a–c*). Such NO release was not affected by rtPA, but was attenuated by PAI-1 (Fig. 4*a*). In tPA-null cultures, the NO release produced by NMDA was attenuated, but it was augmented by rtPA, an effect blocked by PAI-1 (Fig. 4*a*). These observations, collectively, indicate that tPA modulates the NO release produced by activation of NMDA receptors.

tPA Does Not Influence NMDA-Induced Currents and Intracellular Ca^{2+} Rise. tPA could facilitate NO synthesis by augmenting NMDA receptor currents and the resulting rise in intracellular Ca^{2+} (13). Such enhanced increase in Ca^{2+}, in turn, would lead to greater activation of nNOS, a Ca^{2+}-calmodulin-dependent enzyme. To test this hypothesis, we examined NMDA receptor currents in neuronal cultures from wild-type and tPA-null mice. Surprisingly, the currents evoked by NMDA were larger in tPA-null neurons, not smaller as predicted (Fig. 4*b*). rtPA slightly enhanced the current in wild-type cultures, but had no effect in tPA-null cultures (Fig. 4*b*). We then used the Ca^{2+} indicator fura-2 to examine the changes in cytoplasmic free Ca^{2+} produced by NMDA. Like NMDA currents, the increase in intracellular Ca^{2+} induced by NMDA was larger in tPA-null neurons and was not altered by rtPA (Fig. 4*c*). Such enhancement of NMDA
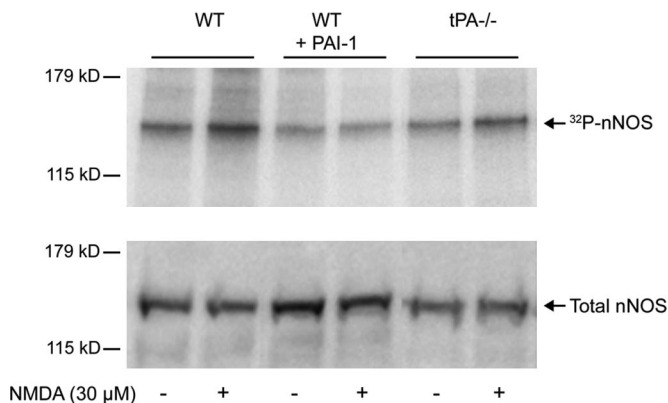
Fig. 5. tPA influences the phosphorylation state of nNOS. Autoradiogram of SDS/PAGE of immunoprecipitated ^{32}P-nNOS in cultured cortical neurons. (*Upper*) PAI-1-treated (1 μg/ml) wild-type neurons and tPA$^{-/-}$ neurons showed decreased nNOS phosphorylation compared with untreated wild-type controls and displayed a reduced phosphorylation response to NMDA (30 μM). (*Lower*) Western blot showing total nNOS levels in identically treated cortical cultures.

currents and Ca^{2+} increase may reflect compensatory changes resulting from lack of tPA. Therefore, tPA does not promote NO synthesis by enhancing the intracellular Ca^{2+} rise evoked by NMDA receptor activation.

tPA Is Required for NMDA Receptor-Induced nNOS Phosphorylation.
The observation that the effect of tPA on NO release is independent of NMDA receptor currents and intracellular Ca^{2+}, raises the possibility that tPA regulates the coupling between NMDA receptors and nNOS. Phosphorylation of nNOS has emerged as an important regulator of its enzymatic activity (28, 30). In particular, glutamatergic stimulation of cultured cortical neurons results in a NMDA receptor-dependent increase in nNOS phosphorylation, which is associated with heightened enzymatic activity (30). Therefore, we used cortical neuronal cultures to investigate whether tPA influences nNOS phosphorylation. In the resting state, nNOS phosphorylation was reduced in wild-type neurons pretreated with PAI-1 (1 μg/ml) ($-37 \pm 7\%$; $P < 0.05$; $n = 4$) (Fig. 5). After treatment with NMDA, wild-type neurons displayed an increase in nNOS phosphorylation compared with untreated controls ($+29 \pm 5\%$; $P < 0.05$). In contrast, NMDA failed to increase nNOS phosphorylation in PAI-1-treated neurons ($P > 0.05$ from control) (Fig. 5). Similar results were obtained with tPA-null cultures (Fig. 5). Considering that NMDA-induced nNOS phosphorylation increases nNOS activity (30), these results suggest that the effect of tPA on the NO release induced by NMDA (Fig. 4a) involves modulation of nNOS phosphorylation in the resting state and during NMDA receptor activation.

Discussion

We have demonstrated that tPA is essential for the increase in CBF evoked by neural activity, but not for the hyperemic response produced by other vasoactive stimuli. In particular, tPA is selectively involved in the NMDA-dependent component of functional hyperemia, an effect mediated by enhancing the coupling between NMDA receptor activity and synthesis of neuronal NO. The effect of tPA could not be accounted for by an increase in Ca^{2+} fluxes through the NMDA receptor (13), because NMDA currents and the associated rise in intracellular Ca^{2+} are not attenuated in tPA-null neurons. Rather, tPA enables NMDA-dependent NO production by influencing the phosphorylation state of nNOS and leading to increased enzymatic activity. These findings, collectively, support the hypoth-

esis that tPA regulates the coupling between NMDA receptor activation and NO-dependent functional hyperemia by modulating nNOS phosphorylation. nNOS-derived NO could contribute to the increase in CBF by acting directly on local arterioles or by evoking the release of vasoactive mediators from astrocytes (22).

The NMDA receptor is structurally and functionally linked to nNOS via PSD-95 (27, 43). This ternary complex enables nNOS to be efficiently and selectively activated by the influx of calcium through the NMDA receptor. Phosphorylation constitutes an important regulatory mechanism for nNOS activity (28, 30). In agreement with previous results (30), we found that nNOS phosphorylation is rapidly increased after NMDA receptor activation. However, in the absence of tPA or after pretreatment with PAI-1, NMDA-induced nNOS phosphorylation is not as pronounced as in control neurons. Furthermore, we found that tPA also exerts an influence on basal NOS phosphorylation. Given that NMDA-induced NO synthesis is reduced in tPA-null neurons or in PAI-1-treated wild-type neurons, our results support a role for tPA in the NMDA-induced phosphorylation of nNOS, and, consequently, in the regulation of nNOS catalytic activity during postsynaptic NMDA receptor activation.

Although tPA has been strongly implicated in the modulation of NMDA receptor function, the underlying mechanisms remain unclear (6). tPA is stored in synaptic secretory vesicles and is released into the extracellular space in response to neuronal depolarization (7). Astrocytes are also a source of tPA (6). Extracellularly released tPA has been shown to interact directly with the NMDA receptor (13, 15). Such interaction could modulate downstream kinases and phosphatases that regulate nNOS activity via phosphorylation (30). The major kinases and phosphatases involved in NMDA-induced nNOS phosphorylation include protein phosphatase 1, calcineurin, Ca^{2+}-calmodulin kinase II, and Akt (30). Their role in the effects of tPA will be addressed in future studies. tPA could also interact with the lipoprotein receptor-related protein 1 (LRP-1), which is linked with PSD-95 and can modulate NMDA receptor signaling through activation of protein kinase A (44). Whatever the interaction between tPA and the NMDA receptor, our data suggest that regulation of nNOS phosphorylation is involved in the effect of tPA on NO production.

The NMDA receptor is essential for normal brain function, and NO is a critical link in its signaling pathways (45, 46). Our findings demonstrate that tPA is a key regulator of the coupling between NMDA receptor activity and NO synthesis and, as such, is indispensable for the normal functions of the NMDA receptor. This conclusion is supported by the findings that both tPA and NO are involved in processes mediated by NMDA receptors, such as synaptic plasticity (10, 14, 47, 48) and, as shown here, functional hyperemia. In diseases associated with excessive glutamate release, overactivation of the NMDA receptor leads to the synthesis of toxic levels of NO, which contribute to neurotoxicity (49). Therefore, the present data also suggest that the well established participation of tPA in neurotoxicity (50, 51) may involve the link between NMDA receptors and nNOS, a hypothesis supported by recent findings in a model of excitotoxic brain injury (52).

The finding that tPA modulates functional hyperemia raises the possibility that tPA deficiency contributes to the alterations in neurovascular coupling that occur in brain pathologies such as ischemic stroke or Alzheimer's disease (AD) (19). Stroke leads to a profound alteration in neurovascular coupling in the acute phase after the ischemic event, which worsens cerebral perfusion and may contribute to brain damage in the ischemic penumbra (53). Considering that cerebral ischemia reduces tPA (54), our data suggest that such reduction could play a role in postischemic neurovascular dysregulation. Furthermore, recent evidence indicates that cerebro-

vascular dysfunction contributes to the pathogenesis of AD (19). Functional hyperemia is attenuated both in mouse models of AD and in AD patients (19, 32). These cerebrovascular alterations occur early in the course of the disease, suggesting a pathogenic role in the development of the cognitive deficits (19). Our data suggest that a deficiency in tPA activity, which has been observed in mouse models of AD (55), could play a role in these neurovascular alterations. Reduced tPA expression and activity in AD could down-regulate NMDA-induced NO synthesis and mediate the attenuation in functional hyperemia and other deficits of NMDA receptor function observed in the disease. Therefore, the link between tPA and NMDA receptor-induced NO release may be crucial not only for its role in the delicate balance between brain activity and cerebral blood supply, but also for the brain dysfunction resulting from the dysregulation of this critical homeostatic mechanism.

Methods

Mice. All procedures were approved by the Institutional Animal Care and Use Committee of Weill Cornell Medical College. Studies were conducted in C57BL/6J mice (The Jackson Laboratory) and in mice lacking tPA or plg (31, 34). Null mice were backcrossed to the C57BL/6J strain for at least nine generations and were obtained from in-house colonies. All mice were 2–3 months of age.

General Surgical Procedures. Mice were anesthetized with isoflurane (maintenance, 2%), intubated, and artificially ventilated (SAR-830; CWE) (32, 33). The femoral vessels were cannulated for recording of arterial pressure, and blood sample collection. Rectal temperature was maintained at 37°C. After surgery, isoflurane was gradually discontinued and anesthesia was maintained with urethane (750 mg/kg, i.p.) and α-chloralose (50 mg/kg, i.p.) (32, 33).

CBF and Cerebrovascular Reactivity. The parietal cortex was exposed (2 × 2 mm), the dura was removed, and the site was superfused with a modified Ringer's solution (37°C; pH 7.3–7.4) (32, 33). CBF was monitored in the window by using a laser Doppler flowmeter (Vasamedic), which detects microvascular blood flow in a 1-mm³ tissue volume (56). The outputs of the flowmeter and blood pressure transducer were connected to a computerized data acquisition system (MacLab). CBF was expressed as percent increase relative to the resting level (32, 33). Experiments were started when arterial pressure and blood gases were in a steady state (mean arterial pressure, 80–90 mmHg; pCO_2, 32–35 mmHg; pO_2, 120–140 mmHg; pH 7.3–7.4). The cranial window was first superfused with a modified Ringer's solution (32, 33), and CBF responses to whisker stimulation were recorded. The whiskers were gently stroked for 60 s with a cotton-tipped applicator. In some mice, acetylcholine (10 μM; Sigma), bradykinin (50 μM; Sigma), the calcium ionophore A23187 (3 μM; Sigma), NMDA (10–80 μM; Sigma), AMPA (2–20 μM), or kainate (2–20 μM) was topically superfused on the cranial window. CBF responses to the NO donor SNAP (50 μM; Sigma) and to the NO-independent vasodilator adenosine (400 μM; Sigma) were also tested. In other experiments, CBF responses were tested before and 30 min after superfusion of the cranial window with MK801 (10 μM), rtPA (20 μg/ml), or PAI-1 (1 μg/ml). The efficacy of the penetration of tPA into the neocortex was confirmed by using *in situ* zymography (SI Fig. 11). In studies in which the tat-conjugated peptide NR2B9c (NH$_2$-YGRKKRRQR-RRKLSSIESDV-CONH$_2$; BIO-SYNTHESIS) or a mutated version that does not interact with NR2 (scNR2B9c) (NH$_2$-YGRKKRRQRRRSVDSSIELK-CONH$_2$) were studied, CBF responses were tested before and 30 min after topical superfusion with the peptide (1 μM). Brain penetration of the peptide was verified by superfusion with NR2B9c carrying a fluorescent tag (data not shown).

Electrocorticogram and Field Potentials. Mice were anesthetized and surgically prepared as described above. The electrocorticogram was recorded by using bipolar recording electrodes positioned stereotaxically on the left somatosensory cortex (3 mm lateral and 1.5 mm caudal to bregma; depth of 0.6 mm) (57). The electrocorticogram was recorded for five epochs each lasting 5 min and separated by a 20-min interval. The timing of the recordings relative to the administration of anesthesia was identical for all animals. Signals were amplified, digitized, and stored (PowerLab; AD Instruments). Spectral analysis of the EEG was performed by using a software module embedded in PowerLab. Field potentials were recorded by using an electrode placed in the somatosensory cortex contralateral to the activated whiskers. The somatosensory

cortex was activated by electrical stimulation of the whisker pad (2 V; 0.5 Hz; pulse duration, 1 ms). Analyses were performed on the average of 10 stimulation trials (33).

Assessment of Cytoplasmic Ca^{2+}. Cytoplasmic free Ca^{2+} was measured by using fura-2 as indicator (Molecular Probes), as previously described (58). Mixed neocortical cultures (days *in vitro* 11–13) from 16- to 17-day-old mouse embryos seeded on polyornithine-coated glass coverslips were loaded with the dye (2 μM) added directly to the culture medium for 45 min at 37°C (59). Coverslips were mounted in a perfusion chamber and placed on a heated (30°C) microscope stage. Images were acquired on a Nikon inverted microscope by using a fluorite oil-immersion lens (Nikon CF UV-F X40; N.A., 1.3). Fura-2 was alternately excited through narrow bandpass filters (340 ± 7.5 and 380 ± 10 nm). An intensified CCD camera (Retiga ExI) recorded the fluorescence emitted by the indicator (510 ± 40 nm). Fluorescent images were digitized and backgrounds were subtracted. Eight to 20 neurons, identified by morphological criteria and by their response to NMDA, were simultaneously recorded in a randomly selected field. Fluorescence measurements were obtained from cell somata, and ratios were calculated for each pixel by using a standard formula (58). Results were expressed as 340/380-nm ratio. NMDA (30 μM) was superfused for 5 min and then washed away.

NO Electrode. Amperometric detection of NO release from neuronal cultures was performed by using an Apollo 4000 Analyzer equipped with an NO-sensitive electrode (tip diameter, 0.1 μm; ISO-NOPNM; World Precision Instruments). The NO detection limit of the electrode is 0.5 nM with a response <3 s. After calibration of the electrode with the NO donor SNAP, NO release triggered by NMDA in cultured cortical neurons was measured. Cultures were perfused with Mg^{2+}-free Hepes extracellular buffer at room temperature. Perfusion of the extracellular buffer was discontinued, and the tip of the electrode was placed close to the neurons. After stabilization of basal NO levels, NMDA (30 μM) was applied to the extracellular buffer and the release of NO from the neurons was monitored for at least 12 min. After the wash, NO release returned to baseline, and neurons were treated with tPA (20 μg/ml) or tPA plus PAI-1 (1 μg/ml) for 10 min. Then, the effects of NMDA application were retested in the same group of neurons. The data were digitally acquired and stored for off-line analysis.

Measurement of NMDA Currents. Whole-cell patch-clamp recordings were conducted at room temperature (22–25°C) in the same cultures used for NO release and fura-2 studies by using an Axopatch 200A amplifier (Axon Instruments) as previously described (58). For NMDA current recordings, the extracellular solution also contained tetrodotoxin (1 μM), nifedipine (1 μM), and 6-cyano-7-nitroquinoxaline-2,3-dione (10 μM). The pClamp 8.01 system (Axon) was used for data acquisition and analysis. NMDA-elicited inward currents were induced from the holding potential of -60 mV, close to the physiological resting potential level. The NMDA current was induced by NMDA (30 μM), and its pure inward peak current was determined by subtracting the background current recorded in the absence of the ligand or drugs. The ratio of currents was recorded with and without drugs as a function of time. PAI-1 (1 μg/ml) or tPA (20 μg/ml) was dissolved in the extracellular solution and superfused for 10 min before testing NMDA currents.

***In Situ* Zymography.** Brains were removed at the time of killing, marked at the site of rtPA superfusion, and frozen at -80°C (15). Sections (20 μM) were cut through the perfusion site and mounted on microscope slides. A fresh casein gel was prepared with plg (50 μg/ml) and overlaid on sections with a coverslip. Overlays were allowed to develop at 37°C in a humidified chamber for 8 h. Zymographic lysis of casein produces a dark zone of tPA activity on a light background when viewed by using dark-field microscopy.

nNOS Phosphorylation. Cultured cortical neurons from wild-type and tPA-null embryos were washed and incubated in assay buffer (130 mM NaCl, 1.8 mM CaCl$_2$, 0.01 mM glycine, 20 mM glucose, 10 mM Hepes, 3 mM KHCO$_3$, pH 7.4) for 30 min at 37°C. Cultures were incubated with [^{32}P]orthophosphate [260 μCi/ml (1 Ci = 37 GBq); GE Healthcare] and with PAI-1 (1 μg/ml; ADI) for 30 min at 37°C. After a 5-min incubation with NMDA (30 μM), cultures were washed twice and lysed for 20 min on ice in RIPA buffer (150 mM NaCl/50 mM Tris·HCl, pH 7.2/1% Triton X-100/1% sodium deoxycholate/ 0.1% SDS) supplemented with protease and phosphatase inhibitor mixture tablets (Roche). Lysates were spun in a microcentrifuge for 10 min at full speed. To immunoprecipitate nNOS, equivalent amounts of supernatant were combined with 1.3 μg of anti-nNOS rabbit polyclonal antibody (Biomol), followed by incubation with protein A-Sepharose 4B Fast Flow

(Sigma). Beads were washed four times with RIPA buffer and prepared in sample buffer, followed by 7.5% SDS/PAGE. Gels were visualized by autoradiography.

Data Analysis. Data are expressed as mean ± SEM. Two-group comparisons were analyzed by the two-tailed *t* test. Multiple comparisons were evaluated by ANOVA and Tukey's test, as appropriate. Statistical significance was considered for $P < 0.05$.

1. Collen D, Lijnen HR (2004) *J Thromb Haemost* 2:541–546.
2. Huber K (2001) *J Thromb Thrombolysis* 11:183–193.
3. Levin EG, del Zoppo GJ (1994) *Am J Pathol* 144:855–861.
4. Marler JR, Goldstein LB (2003) *Science* 301:1677.
5. Huber K, Christ G, Wojta J, Gulba D (2001) *Thromb Res* 103(Suppl 1):S7–S19.
6. Samson AL, Medcalf RL (2006) *Neuron* 50:673–678.
7. Lochner JE, Honigman LS, Grant WF, Gessford SK, Hansen AB, Silverman MA, Scalettar BA (2006) *J Neurobiol* 66:564–577.
8. Gualandris A, Jones TE, Strickland S, Tsirka SE (1996) *J Neurosci* 16:2220–2225.
9. Zhuo M, Holtzman DM, Li Y, Osaka H, DeMaro J, Jacquin M, Bu G (2000) *J Neurosci* 20:542–549.
10. Huang YY, Bach ME, Lipp HP, Zhuo M, Wolfer DP, Hawkins RD, Schoonjans L, Kandel ER, Godfraind JM, Mulligan R, *et al.* (1996) *Proc Natl Acad Sci USA* 93:8699–8704.
11. Mataga N, Nagai N, Hensch TK (2002) *Proc Natl Acad Sci USA* 99:7717–7721.
12. Schaefer U, Machida T, Vorlova S, Strickland S, Levi R (2006) *J Exp Med* 203:2191–2200.
13. Nicole O, Docagne F, Ali C, Margaill I, Carmeliet P, MacKenzie ET, Vivien D, Buisson A (2001) *Nat Med* 7:59–64.
14. Centonze D, Napolitano M, Saulle E, Gubellini P, Picconi B, Martorana A, Pisani A, Gulino A, Bernardi G, Calabresi P (2002) *Eur J Neurosci* 16:713–721.
15. Pawlak R, Melchor JP, Matys T, Skrzypiec AE, Strickland S (2005) *Proc Natl Acad Sci USA* 102:443–448.
16. Armstead WM, Cines DB, Al-Roof Higazi A (2004) *J Neurotrauma* 21:1204–1211.
17. Cipolla MJ, Lessov N, Clark WM, Haley EC, Jr (2000) *Stroke* 31:940–945.
18. Nassar T, Akkawi S, Shina A, Haj-Yehia A, Bdeir K, Tarshis M, Heyman SN, Higazi AA (2003) *Blood* 103:897–902.
19. Iadecola C (2004) *Nat Rev Neurosci* 5:347–360.
20. Lauritzen M, Gold L (2003) *J Neurosci* 23:3972–3980.
21. Raichle ME, Mintun MA (2006) *Annu Rev Neurosci* 29:449–476.
22. Iadecola C, Nedergaard M (2007) *Nat Neurosci* 10:1369–1376.
23. Gsell W, Burke M, Wiedermann D, Bonvento G, Silva AC, Dauphin F, Buhrle C, Hoehn M, Schwindt W (2006) *J Neurosci* 26:8409–8416.
24. Rancillac A, Rossier J, Guille M, Tong XK, Geoffroy H, Amatore C, Arbault S, Hamel E, Cauli B (2006) *J Neurosci* 26:6997–7006.
25. Buerk DG, Ances BM, Greenberg JH, Detre JA (2003) *NeuroImage* 18:1–9.
26. Bredt DS, Snyder SH (1990) *Proc Natl Acad Sci USA* 87:682–685.
27. Christopherson KS, Hillier BJ, Lim WA, Bredt DS (1999) *J Biol Chem* 274:27467–27473.
28. Bredt DS, Ferris CD, Snyder SH (1992) *J Biol Chem* 267:10976–10981.
29. Hayashi Y, Nishio M, Naito Y, Yokokura H, Nimura Y, Hidaka H, Watanabe Y (1999) *J Biol Chem* 274:20597–20602.
30. Rameau GA, Tukey DS, Garcin-Hosfield ED, Titcombe RF, Misra C, Khatri L, Getzoff ED, Ziff EB (2007) *J Neurosci* 27:3445–3455.
31. Carmeliet P, Schoonjans L, Kieckens L, Ream B, Degen J, Bronson R, De Vos R, van den Oord JJ, Collen D, Mulligan RC (1994) *Nature* 368:419–424.
32. Niwa K, Younkin L, Ebeling C, Turner SK, Westaway D, Younkin S, Ashe KH, Carlson GA, Iadecola C (2000) *Proc Natl Acad Sci USA* 97:9735–9740.
33. Kazama K, Wang G, Frys K, Anrather J, Iadecola C (2003) *Am J Physiol* 285:H1890–H1899.
34. Ploplis VA, Carmeliet P, Vazirzadeh S, Van Vlaenderen I, Moons L, Plow EF, Collen D (1995) *Circulation* 92:2585–2593.
35. Hoffmeyer HW, Enager P, Thomsen KJ, Lauritzen MJ (2007) *J Cereb Blood Flow Metab* 27:575–587.
36. Faraci FM, Breese KR (1993) *Circ Res* 72:476–480.
37. Northington FJ, Tobin JR, Koehler RC, Traystman RJ (1995) *Am J Physiol* 269:H215–H221.
38. Pelligrino DA, Gay RL, Baughman VL, Wang Q (1996) *Am J Physiol* 271:H990–H995.
39. Brenman JE, Chao DS, Gee SH, McGee AW, Craven SE, Santillano DR, Wu Z, Huang F, Xia H, Peters MF, *et al.* (1996) *Cell* 84:757–767.
40. Migaud M, Charlesworth P, Dempster M, Webster LC, Watabe AM, Makhinson M, He Y, Ramsay MF, Morris RG, Morrison JH, *et al.* (1998) *Nature* 396:433–439.
41. Sattler R, Xiong Z, Lu WY, Hafner M, MacDonald JF, Tymianski M (1999) *Science* 284:1845–1848.
42. Aarts M, Liu Y, Liu L, Besshoh S, Arundine M, Gurd JW, Wang YT, Salter MW, Tymianski M (2002) *Science* 298:846–850.
43. Bredt DS, Snyder SH (1989) *Proc Natl Acad Sci USA* 86:9030–9033.
44. Herz J, Strickland DK (2001) *J Clin Invest* 108:779–784.
45. Mungrue IN, Bredt DS (2004) *J Cell Sci* 117:2627–2629.
46. Pacher P, Beckman JS, Liaudet L (2007) *Physiol Rev* 87:315–424.
47. Pang PT, Teng HK, Zaitsev E, Woo NT, Sakata K, Zhen S, Teng KK, Yung WH, Hempstead BL, Lu B (2004) *Science* 306:487–491.
48. Son H, Hawkins RD, Martin K, Kiebler M, Huang PL, Fishman MC, Kandel ER (1996) *Cell* 87:1015–1023.
49. Keynes RG, Garthwaite J (2004) *Curr Mol Med* 4:179–191.
50. Wang YF, Tsirka SE, Strickland S, Stieg PE, Soriano SG, Lipton SA (1998) *Nat Med* 4:228–231.
51. Armstead WM, Nassar T, Akkawi S, Smith DH, Chen XH, Cines DB, Higazi AA (2006) *Nat Neurosci* 9:1150–1155.
52. Parathath SR, Parathath S, Tsirka SE (2006) *J Cell Sci* 119:339–349.
53. Kunz A, Park L, Abe T, Gallo EF, Anrather J, Zhou P, Iadecola C (2007) *J Neurosci* 27:7083–7093.
54. Hosomi N, Lucero J, Heo JH, Koziol JA, Copeland BR, del Zoppo GJ (2001) *Stroke* 32:1341–1348.
55. Melchor JP, Pawlak R, Strickland S (2003) *J Neurosci* 23:8867–8871.
56. Lindsberg P, O'Neill J, Paakkari I, Hallembeck J, Feuerstein G (1989) *Am J Physiol* 257:H674–H680.
57. Park L, Anrather J, Zhou P, Frys K, Wang G, Iadecola C (2004) *Arterioscler Thromb Vasc Biol* 24:1860–1865.
58. Kawano T, Anrather J, Zhou P, Park L, Wang G, Frys KA, Kunz A, Cho S, Orio M, Iadecola C (2006) *Nat Med* 12:225–229.
59. Lesuisse C, Martin LJ (2002) *J Neurobiol* 51:9–23.